

Article

Surfactant-Assisted Label-Free Fluorescent Aptamer Biosensors and Binding Assays

Hanxiao Zhang , Albert Zehan Li and Juewen Liu * 

Department of Chemistry, Waterloo Institute for Nanotechnology, University of Waterloo, Waterloo, ON N2L 3G1, Canada

* Correspondence: liujw@uwaterloo.ca

Abstract: Using DNA staining dyes such as SYBR Green I (SGI) and thioflavin T (ThT) to perform label-free detection of aptamer binding has been performed for a long time for both binding assays and biosensor development. Since these dyes are cationic, they can also adsorb to the wall of reaction vessels leading to unstable signals and even false interpretations of the results. In this work, the stability of the signal was first evaluated using ThT and the classic adenosine aptamer. In a polystyrene microplate, a drop in fluorescence was observed even when non-binding targets or water were added, whereas a more stable signal was achieved in a quartz cuvette. Equilibrating the system can also improve signal stability. In addition, a few polymers and surfactants were also screened, and 0.01% Triton X-100 was found to have the best protection effect against fluorescence signal decrease due to dye adsorption. Three aptamers for Hg^{2+} , adenosine, and cortisol were tested for their sensitivity and signal stability in the absence and presence of Triton X-100. In each case, the sensitivity was similar, whereas the signal stability was better for the surfactant. This study indicates that careful control experiments need to be designed to ensure reliable results and that the reliability can be improved by using Triton X-100 and a long equilibration time.

Keywords: aptamers; biosensors; surfactant; fluorescence



Citation: Zhang, H.; Li, A.Z.; Liu, J. Surfactant-Assisted Label-Free Fluorescent Aptamer Biosensors and Binding Assays. *Biosensors* **2023**, *13*, 434. <https://doi.org/10.3390/bios13040434>

Received: 26 February 2023

Revised: 27 March 2023

Accepted: 27 March 2023

Published: 29 March 2023



Copyright: © 2023 by the authors. Licensee MDPI, Basel, Switzerland. This article is an open access article distributed under the terms and conditions of the Creative Commons Attribution (CC BY) license (<https://creativecommons.org/licenses/by/4.0/>).

1. Introduction

Developing assays to study aptamer binding is of great importance to validate newly selected aptamers, characterize aptamer binding, and design biosensors [1–5]. Among the numerous aptamer binding assays [6–9], those based on DNA staining dyes such as SYBR Green I, thioflavin T, and thiazole orange have been very popular [10–15] due to their label-free nature and cost-effectiveness. In a typical assay, a dye and an aptamer are mixed, and their fluorescence is monitored as a function of the target analyte concentration. The assumption is that aptamer–target binding can either promote dye binding or displace the dye, leading to increased or decreased fluorescence, respectively [13]. Another popular label-free method is to use citrate-capped gold nanoparticles. However, our recent studies indicated that gold nanoparticles can strongly adsorb various target molecules, which can mislead the interpretation of assay results [16,17]. In this regard, the dye-staining assay is relatively more reliable.

However, the dye-staining assay also has complications. First, it may not work for all aptamers and the applicability of the assay is a trial-and-error process. Sometimes, the change in fluorescence is very small, which can compromise the reliability of this method and make quantitative measurement difficult. For many such assays, the fluorescence intensity drops when target molecules are added and the change in fluorescence intensity is within one-fold, such as in the adenosine aptamer with ThT [18–21]. Therefore, it is important that the observed fluorescence drop is due to aptamer binding. To ensure this, it is critical to ensure a stable fluorescence signal before titrating target molecules. Since DNA staining dyes are mostly cationic, they can be adsorbed by sample containers such as glass

cuvettes and plastic microplates that have negatively charged surfaces [22,23]. This type of adsorption interaction may strongly interfere with the assay and even cause false signals.

In this study, we studied the signal stability problem and explored two methods to establish stable background fluorescence. The first method is simply to wait for the signal to stabilize before titrating target molecules, where we observed time-dependent signal change even without adding target molecules. The second method is to add surfactants to cover the surface of reaction vessels. For this, we screened various surfactants and demonstrated the stabilization effect of Triton X-100 for a few representative aptamers.

2. Materials and Methods

2.1. Chemicals

All of the DNA samples were ordered from Integrated DNA Technologies (Coralville, IA). The DNA sequences and modifications used are in Table 1. Surfactant, mercury acetate, SYBR Green I (SGI), thioflavin T (ThT), adenosine (ADE), and cortisol were purchased from Sigma-Aldrich. Half-area black 96-well microplates and human AB serum were purchased from Corning and Greiner. Quartz fluorescence cuvettes were purchased from Agilent. Several buffers were prepared. Buffer 1 (for most adsorption studies and Ade aptamer): 50 mM pH 7.6 Tris, 500 mM NaCl, 20 mM MgCl₂. Buffer 2 (for T₃₀ Hg²⁺ binding DNA): 20 mM pH 7.5 MOPS. Buffer 3 (for CSS.1-42 aptamer): 20 mM pH 7.5 HEPES, 100 mM NaCl, 10 mM MgCl₂. Buffer 4 (for Ade and Ade-M2 aptamer): 10 mM HEPES buffer, pH 7.6, 50 mM NaCl, and 4 mM MgCl₂. Buffer 5 (for Ade aptamer): 10 mM HEPES buffer, pH 7.6, 50 mM NaCl, 4 mM MgCl₂, and 5% human AB serum.

Table 1. DNA sequences and modifications used in this work.

Name	Sequences (5'-3')
DNA1	ACGACACGGAGGCTTAGTTTGCTAAATGGTCATGTCGT
CSS.1-42	GACGACGCCCGCATGTTCCATGGATAGTCTTGACTAGTCGTC
Ade Apt	ACCTGGGGGAGTATTGCCGAGGAAGGT
Ade Apt M2	ACCTGGGGTAGTATTGCCGAGTAAGGT
T ₃₀	TTTTTTTTTTTTTTTTTTTTTTTTTTTTTTTTTTTT

2.2. Effect of Time-Dependent Stabilization

Time-dependent stabilization was evaluated using a 96-well black plate. The sample solutions contained 100 nM adenosine aptamer or Ade-M2 aptamer and 2 μM ThT in Buffer 4 or Buffer 5 (when testing the effect of 5% serum on the titration of the adenosine aptamer by adenosine). Fluorescence intensity was monitored at 420 nm excitation and 490 nm emission using a Horiba Fluoromax 4 fluorometer (500 μL, cuvette-based) maintained at 20 °C by a water bath or a Tecan Spark plate reader (100 μL, plate-based). Adenosine, guanosine, and MilliQ water were gradually titrated up to a final target concentration of 500 μM. Titration was either performed immediately or equilibrated by waiting for 10 min to reach a stable baseline before titration.

2.3. Test of Different Surfactants and Assay Materials

The protective effects of different surfactants were evaluated using a 96-well black plate (Corning). The sample solution (100 μL) contained 200 nM DNA1 aptamer, 0.02 × SGI in Buffer 1 with different concentrations of Triton X-100 (0.1%, 0.01%, 0.001%, and 0.0001%). The fluorescence intensity was monitored under excitation at 488 nm and absorption at 532 nm for 30 min using a Tecan Spark plate reader. The effects of different assay materials were tested using 96-well black plates (Corning and Greiner) and a quartz cuvette. To test the effect of different surfactants, a 96-well black plate (Corning) and a quartz cuvette were used. For the plate method, 100 μL of the sample solution contained 200 nM DNA1 aptamer, 0.02 × SGI in Buffer 1, and 0.01% surfactant (Triton X-100, Tween 20, PEG 2000,

PEG 20000, SDS or CTAB). For the cuvette method, 500 μL sample solution contained 1 μM DNA1 aptamer, $0.1 \times$ SGI in Buffer 1, and 0.01% of the various surfactants. To test the influence of Triton X-100 on the adsorption of dyes on sample containers, $0.5 \times$ SGI in Buffer 1 was incubated for 15 min in a 96-well black plate, and then the solution was fully removed. Next (0.01% Triton X-100 or no Triton X-100) in Buffer 1 was added along with a 70-mer double-stranded DNA into the same wells used initially. In clean wells, 70-mer double-stranded DNA, in the presence of 0.01% Triton X-100, was titrated up to a final concentration of 0.4 μM SGI. Fluorescence intensity was monitored using a Tecan Spark plate reader at 488 nm excitation and 532 nm emission.

2.4. Hg^{2+} Sensing Assay

The effect of surfactants on the binding of Hg^{2+} by T_{30} DNA was evaluated using a 96-well black plate (Corning) in Buffer 2 containing 200 nM T_{30} aptamer, $0.1 \times$ SGI, and 0% or 0.01% Triton X-100. The sample solution (100 μL) was titrated with mercury acetate up to a final concentration of 3 μM . Fluorescence intensity was monitored using a Tecan Spark plate reader at 488 nm excitation and 532 nm emission. For signal stability measurement, 100 μL of sample solution contained 200 nM T_{30} aptamer, $0.1 \times$ SGI, 2 μM mercury acetate, and 0% or 0.01% Triton X-100 in Buffer 2. Fluorescence intensity was monitored using the microplate reader with 488 nm excitation and 532 nm emission for 30 min.

2.5. Adenosine Sensing Assay

The effect of surfactants on the binding of adenosine by its aptamer was evaluated using a 96-well black (Corning) plate in Buffer 1 containing 1 μM aptamer, 1 μM ThT, and 0% or 0.01% Triton X-100. The sample solution (100 μL) was titrated with adenosine up to a final concentration of 150 μM . Fluorescence intensity was monitored using the microplate reader at 488 nm excitation and 532 nm emission. For signal stability measurement, 100 μL of sample solution contained, 1 μM aptamer, 100 μM adenosine, 1 μM ThT, and 0% or 0.01% Triton X-100 in Buffer 1. Fluorescence intensity was monitored using the microplate reader with 488 nm excitation and 532 nm emission for 30 min.

2.6. Cortisol Sensing Assay

The effect of surfactants on the binding of cortisol to CSS.1-42 DNA was evaluated using a 96-well black plate (Corning) in Buffer 3 containing 1 μM CSS.1-42 aptamer, $0.1 \times$ SGI, and 0% or 0.01% Triton X-100. The sample solution (100 μL) was titrated with cortisol up to a final concentration of 6 μM . Fluorescence intensity was monitored using the microplate reader at 488 nm excitation and 532 nm emission. For signal stability measurement, 100 μL sample solution contained 1 μM CSS.1-42 aptamer, 5 μM cortisol, $0.1 \times$ SGI, and 0% or 0.01% Triton X-100 in Buffer 3. Fluorescence intensity was monitored using the microplate reader at 488 nm excitation and 532 nm emission for 30 min.

3. Results and Discussion

3.1. Effect of Stabilization in Microplates and Cuvettes

The classic adenosine aptamer stained by ThT was used to study the effect of time-dependent signal stability on the dye staining method [24,25]. A schematic representation of the reaction is shown in Figure 1A. In this case, adenosine binding can displace ThT, resulting in decreased fluorescence [18]. In contrast, non-binding molecules do not displace ThT and no fluorescence drops are expected. For this assumption to be valid, it is important that the fluorescence change is only due to aptamer binding instead of other processes, such as dye adsorption by the assay vessel.

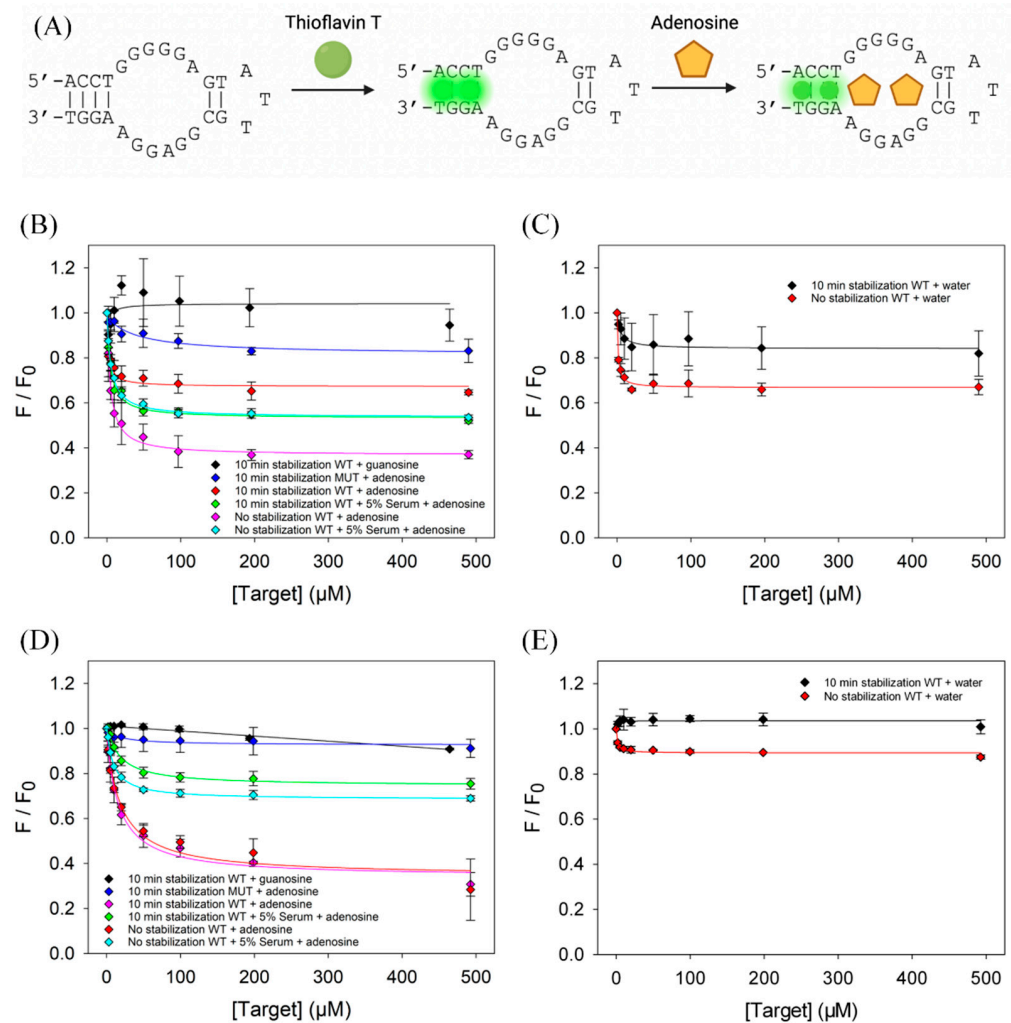


Figure 1. (A) Scheme of adenosine binding to the adenosine aptamer detected by ThT. Initially, ThT binds to the aptamer, producing a strong fluorescence signal. Adenosine binding displaces ThT, resulting in a decrease in fluorescence. Binding assay in a polystyrene microplate by (B) titrating adenosine and guanosine, and (C) titrating water. Binding assay in a quartz cuvette by (D) titrating adenosine and guanosine, and (E) titrating water. WT: wild-type adenosine aptamer; MUT: Ade Apt M2 mutant. Fluorescence intensities were normalized to their respective baseline value (absent of target) before titration.

First, we conducted the titration in a 96-well microplate without waiting (adenosine was titrated immediately after adding the aptamer and ThT mixture). Adding adenosine produced a 65% decrease in this case (magenta line, Figure 1B). Interestingly, only a 35% drop was obtained after incubating the aptamer and ThT for 10 min in the microplate before titration (red line, Figure 1B). However, when the same titration was conducted in 5% serum, a 45% drop was exhibited with and without incubation (green and turquoise lines, Figure 1B). The result suggested that the serum proteins might have blocked the container surface to prevent further adsorption of the dye.

To ensure that the observed fluorescence drop was specific, we performed a control experiment using a mutant (see Table 1 for the sequence named Ade Apt M2, where two guanines of Ade Apt were mutated to thymines) [18], in which only a 15% drop was observed after stabilization (blue line, Figure 1B). In another control experiment, guanosine was added to the wild-type aptamer, and no change in fluorescence was observed (black line, Figure 1B). Guanosine is known to be a nonbinding molecule for this aptamer [24]. This set of control experiments indicated that the aptamer was specifically bound to adenosine.

We then determined the fitted K_d values. In the microplate, the K_d of adenosine binding to the aptamer was $5.0 \pm 2.1 \mu\text{M}$ without stabilization and $2.8 \pm 3.1 \mu\text{M}$ with 10 min stabilization. In 5% serum, the K_d was $5.6 \pm 1.1 \mu\text{M}$ without stabilization and $5.1 \pm 2.0 \mu\text{M}$ with 10 min stabilization. The literature reported K_d for this aptamer is between 6 and 20 μM adenosine [18–20]. Considering the error associated with this method, there was not a significant difference in K_d with or without stabilization, and because all determined K_d are only marginally below the lower bound of the reported K_d , this demonstrates that the ThT-based titration method can provide valuable information on the strength of target binding in this case. In addition, the difference in K_d determined in the presence and absence of 5% serum was negligible, suggesting that this method can retain its accuracy within biological fluids.

As a further control, water was titrated into the aptamer/ThT samples (Figure 1C). The wild-type aptamer titrated with water produced a 20% drop with 10 min stabilization (fitted $K_d = 11 \pm 12$), compared to a 33% drop without stabilization (fitted $K_d = 1.3 \pm 0.3$). This is concerning since in theory water does not impact the aptamer binding to ThT and thus no fluorescence drop should have occurred. This suggests that the system had a time-dependent signal change even without adding target molecules and we reason that two processes occurred simultaneously to contribute to the fluorescence drop: dye adsorption and aptamer binding.

With stabilization, the effect of dye adsorption was minimized. However, without stabilization, the interpretation of the results can be misleading. Despite this, it was still possible to differentiate between binding and non-binding targets based on the results in Figure 1B. Quantitative fitting of the data needs to be careful, since even water produced a similar K_d compared to adenosine.

We then performed the same reactions using a quartz cuvette, which should have lower adsorption because quartz does not have hydrophobic interactions with DNA-staining dyes. In this case, a 60% fluorescence drop was observed upon adenosine binding, regardless of the 10 min stabilization (red and magenta lines, Figure 1D). When the same experiment was performed in 5% serum, there was a 30% drop without stabilization, compared to a 25% drop with stabilization, again suggesting serum proteins may mitigate dye adsorption (green and turquoise lines, Figure 1D). The aptamer titrated with water produced a 13% drop without stabilization and essentially no drop was observed with stabilization (Figure 1E). Using the cuvette method, the K_d of adenosine binding to the aptamer was $16.6 \pm 8.4 \mu\text{M}$ with stabilization and $17.5 \pm 8.7 \mu\text{M}$ without stabilization. In serum, the K_d was $20.9 \pm 2.7 \mu\text{M}$ with stabilization and $9.5 \pm 2.1 \mu\text{M}$ without stabilization. Using ITC, we obtained a K_d of 16.4 μM under similar buffer conditions and DNA samples [26]. In addition, all negative controls generated less than a 15% drop in fluorescence and no clear sign of binding (blue and black lines, Figure 1D). Therefore, quartz cuvettes can generate reliable results for quantitative measurement.

3.2. Time-Dependent Signal Stability

The above studies indicated time-dependent initial fluorescence. We then monitored the kinetics of this initial fluorescence change before titration (Figure 2A). Within 10 min after mixing the aptamer and ThT, the fluorescence in the microplate decreased by 25%, while that in the cuvette decreased by approximately 15%. We attributed this decrease to the adsorption of the dye to the walls of the reaction vessels (Figure 2B). The fluorescence in the cuvette was close to stable at the end of 10 min, but the fluorescence in the microplate continued to decrease. If titration is performed immediately, the observed fluorescence drop is the sum of two processes: aptamer binding and dye adsorption. We also noticed that the amount of fluorescence drop was smaller in the cuvette when guanosine or water was added, compared to the drop seen in Figure 2A, where nothing was added. This could be due to perturbation during addition and mixing, facilitating the systems to equilibrate.

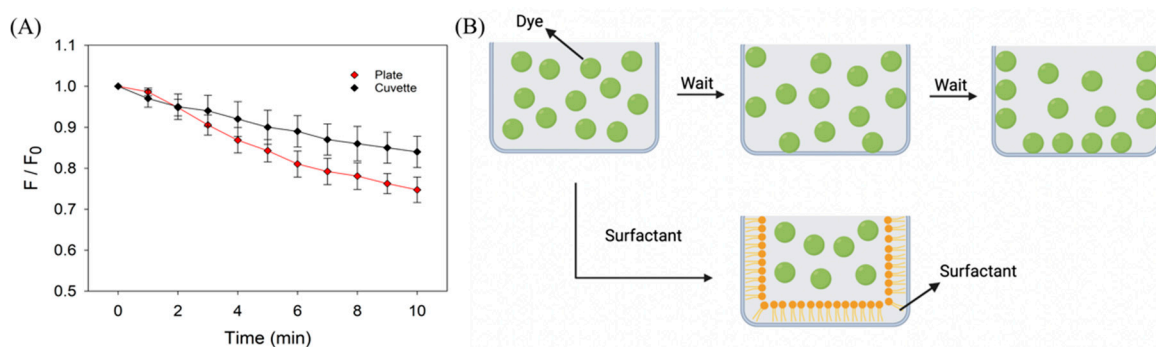


Figure 2. (A) Time-dependent fluorescence intensity of the adenosine aptamer and ThT mixture in a polystyrene microplate and a quartz cuvette. (B) A scheme showing the adsorption of dyes such as SGI and ThT to the wall of a reaction vessel.

In both the plate- and cuvette-based assays, even with stabilization, there was still a fluorescence drop observed between target concentrations of 0–20 μM for non-binding controls (conditions with guanosine, water, or mutant aptamer). It is extremely important to have appropriate controls so that such non-binding events cannot be interpreted as aptamer binding. Overall, for the adenosine aptamer, it was possible to discern binding targets from non-binding targets using this label-free method. With stabilization and in a non-adsorbing vessel, the measured K_d values were more reliable. For the adenosine aptamer with ThT, a fluorescence drop of nearly 60% was achieved. However, in other cases, the fluorescence change produced can be much smaller than that achieved using this adenosine aptamer. Careful controls are even more important for those aptamers with smaller signal changes.

3.3. The Protective Effect of Surfactants

Aside from waiting for stabilization, another method to reduce nonspecific adsorption is to make the vessel surfaces less adsorbing. A surfactant is composed of hydrophilic and hydrophobic groups. After adding a surfactant to the solution, the surfactant may adsorb onto the surface, preventing DNA/dye adsorption and stabilizing the fluorescence of the system. Most aptamers can function in the presence of many surfactants [27]. However, surfactants may also interact with DNA and dyes, thereby influencing signal production. To test the effect of surfactants, we first used DNA1 (a 38-mer DNA) and stained it with SGI dye.

We first screened a few surfactants and polymers [28]. The basic properties of these surfactants are listed in Table 2. Initially, the fluorescence readings of all surfactant samples were between 200 and 400 fluorescence units (FU) (Figure 3A,B) using both the plate and cuvette, except for SDS (close to 0) and CTAB (lower fluorescence). SDS is an anionic surfactant. We hypothesized that SDS may compete with the aptamer for SGI, resulting in a very weak fluorescence signal. Cationic CTAB may compete with SGI for binding with the DNA. The hydrophilic–lipophilic balance (HLB) values of Triton X-100, CTAB, and SDS are 13.5, 21.4, and 40, respectively [29]. These three surfactants have strong hydrophilicity and weak lipophilic interactions. They mainly bind to DNA and dyes through cation/anion interactions. The data shows that Triton X-100 had the most prominent stabilizing effect on the fluorescence intensity of the DNA-SGI system. Triton X-100 is a non-ionic surfactant (Figure 3F), and thus, the absence of electrostatic interactions with DNA or dye may contribute to its good stabilizing effect.

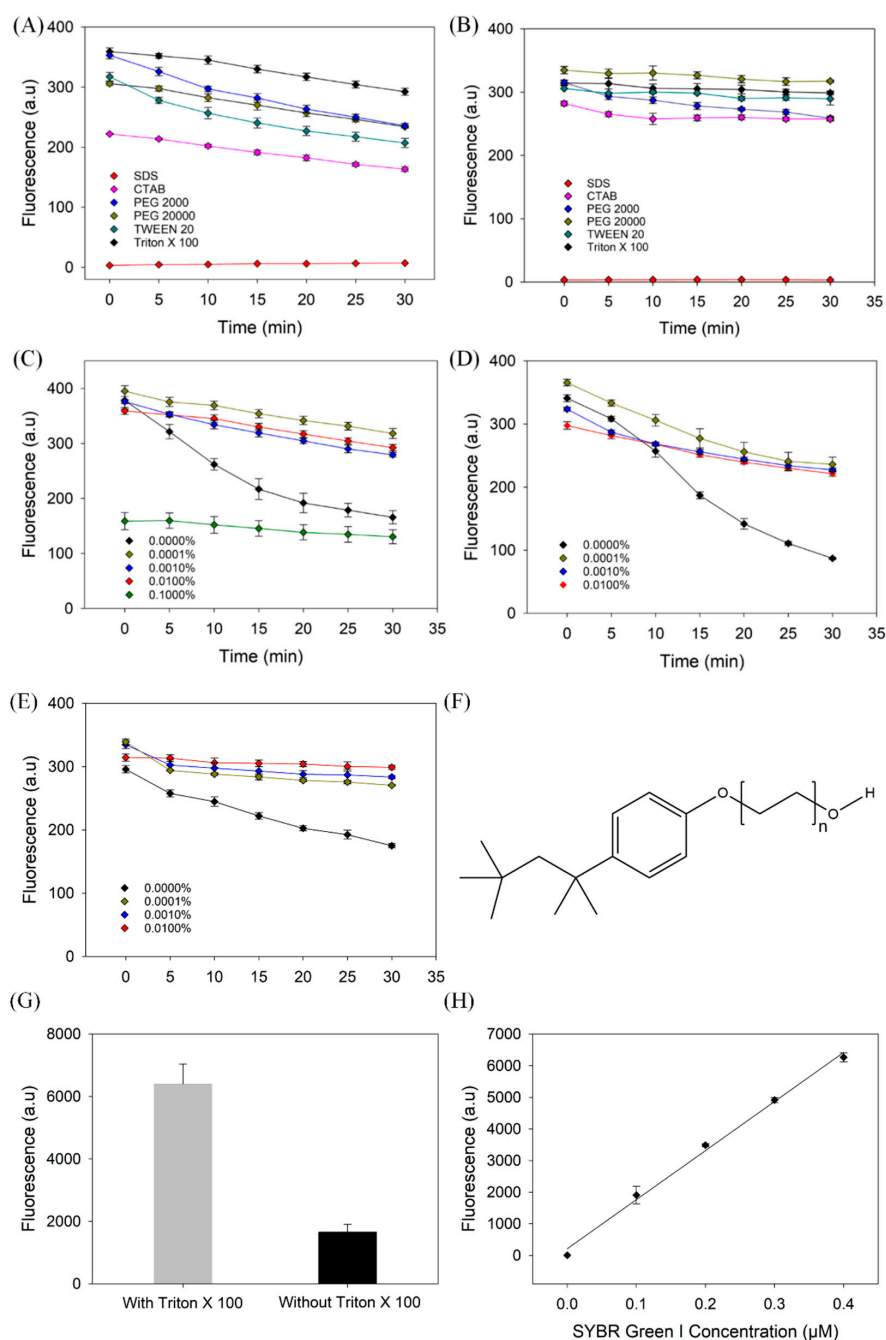


Figure 3. (A) Effect of surfactant on signal stability in Corning 96-well microplate. The samples contained 200 nM DNA1, $0.02\times$ SGI, and 0.01% different surfactants in Buffer 1. (B) Effect of surfactant on signal stability in a quartz cuvette. The solutions contained 1 μM DNA1, $0.1\times$ SGI, and 0.01% different surfactants in Buffer 1. Effect of Triton X-100 concentration on the stability of fluorescence in (C) a Corning microplate, (D) a Greiner microplate, and (E) a quartz cuvette. (F) Structure of Triton X-100. (G) Effect of Triton X-100 on SGI pre-stained microplate well containers. Initially, buffer and 1 μM SGI were incubated for 15 min, then solution was removed. To the same wells, buffer with and without 0.01% Triton X-100 was added alongside 70-mer double-stranded DNA. (H) Titration curve of 70-mer double-stranded DNA titrated by SGI in the presence of 0.01% Triton X-100.

Table 2. Surfactant molecular weights, relevant molar concentrations at 0.01%, and critical micelle concentrations (CMC) [30,31].

Surfactant	Molecular Weight	Concentration at 0.01% (mM)	CMC (mM)
Triton X-100	646.9	0.155	0.19–0.22
TWEEN 20	522.7	0.191	0.046
SDS	288.4	0.347	7.3–8.1
CTAB	364.5	0.274	0.98

We then optimized the concentration of Triton X-100. Initially, the fluorescence intensity produced by the different Triton X-100 concentrations was approximately 400 fluorescence units, except for 0.1% Triton X-100, which had an initial fluorescence of 160 units (Figure 3C). We theorize that because the 0.1% concentration exceeds the critical micelle concentration of Triton X-100 (Table 2), the surfactant may sequester a fraction of SGI to decrease the binding of SGI to the DNA, resulting in a decrease in the fluorescence. It was found that 0.01% Triton X-100 produced the lowest rate of fluorescence decrease, while maintaining a stable fluorescence signal.

To further confirm the adsorption of the dyes and the effect of Triton X-100 on dye adsorption by sample containers, we incubated 1 μM SGI with the microplate in buffers. After removing the solutions, we added buffers with or without Triton X-100 at 0.01% and then added a 70-mer double-stranded DNA to measure the fluorescence intensity, which can reflect the level of adsorption of the pre-adsorbed dyes. The samples containing Triton X-100 were 3.9 times more fluorescent than samples without Triton X-100 (Figure 3G), suggesting that Triton X-100 can prevent SGI adsorption. We explain this phenomenon as Triton X-100 can adsorb on the container wall and displace the SGI adsorbed on the container wall. We then titrated samples containing the dsDNA in 96-well plates using SGI (Figure 3H). An amount of 0.4 μM of SGI was needed to achieve 6300 fluorescence. Thus, about 0.6 μM of SGI was adsorbed to the container wall of a well. We calculated that the container walls absorbed approximately 74% of the SGI.

To test this generality, we further monitored the same DNA in a Greiner microplate (Figure 3D) and a quartz cuvette (Figure 3E). Overall, Triton X-100 exhibited a similar stabilization effect. Comparing the different materials, the rate of fluorescence decrease when using the quartz cuvette was lower than that when using the polystyrene plates. For all samples, 0.01% Triton X-100 was found to be the optimal concentration, which was used in subsequent experiments. The molecular weight of Triton X-100 is 646.9 g/mol, and thus its molar concentration was 0.155 mM. This is far greater than the concentration of aptamer (~ 1 μM). In the following experiments, we used Triton X-100 to further explore the protective effect of surfactants on different aptamers and fluorescent dye conjugates.

3.4. Sensing Mercury Using a Thymine-Rich DNA

We then studied the performance of a few different aptamers under optimized conditions (0.01% Triton X-100). Since the signal variation was more significant in the microplates, we used a microplate for all these experiments. First, we used a T₃₀ DNA for the detection of Hg²⁺ ions as shown in Figure 4A [32]. The fluorescence of the system increases significantly upon binding to Hg²⁺. Regardless of the surfactant, the initial and final fluorescence was comparable. Under the protection of Triton X-100, the fluorescence of the system increased 15.6-fold, although the surfactant-free sample also achieved a 10.0-fold increase (Figure 4B). We studied the stability of the fluorescence signal for samples containing 2 μM Hg²⁺ in a 96-well plate for 30 min (Figure 4C). Without Triton X-100, the fluorescence of the system declined almost linearly as the intensity dropped by 15.2% after 30 min. In the presence of 0.01% Triton X-100, the fluorescence of the system did not change. Evidently, Triton X-100 can achieve a more stable signal, which is very important for accurate analytical results.

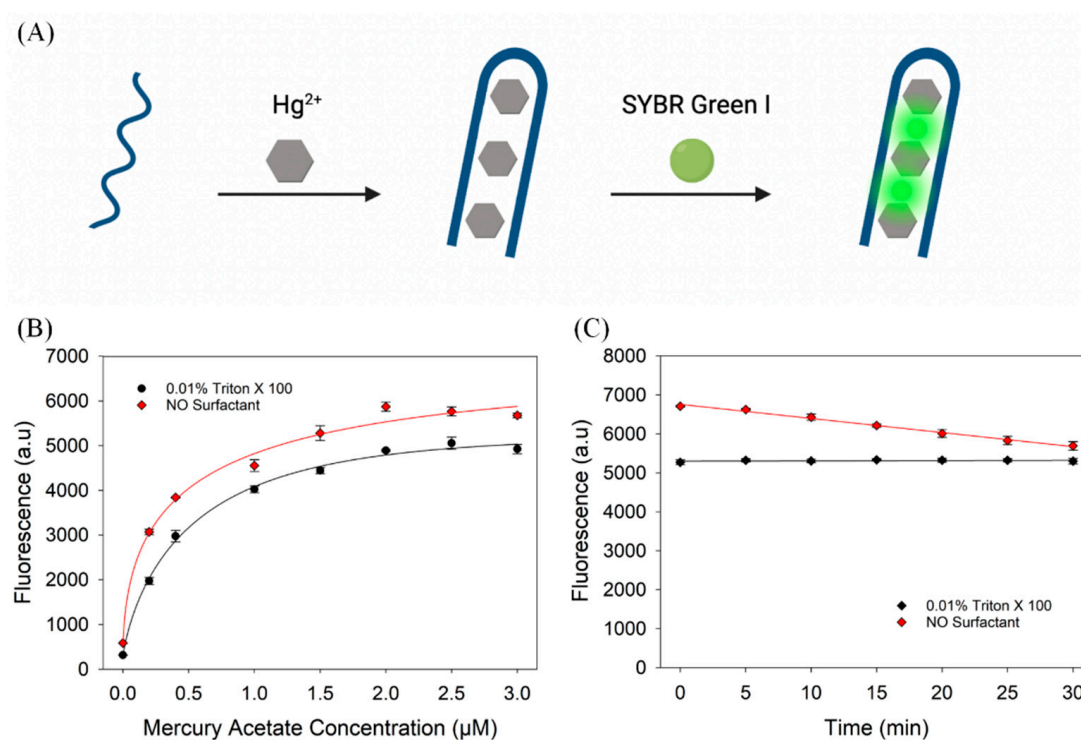


Figure 4. (A) A scheme of Hg^{2+} binding to a thymine-rich DNA detected by SGI. Hg^{2+} binds to the DNA and folds into a structure with a long duplex region, resulting in a strong SGI fluorescence. (B) Titration curve of 200 nM T_{30} using mercury acetate with and without 0.01% Triton X-100. (C) Effect of Triton X-100 on signal stability of T_{30} /SGI in the presence of 2 μM Hg^{2+} .

3.5. Evaluation of the Adenosine Aptamer

The Hg^{2+} binding DNA has a uniquely strong fluorescence enhancement, which is not seen in most other aptamers. For the majority of aptamers, the change in fluorescence is only within one-fold. Thus, we further tested a few small molecule binding aptamers. We first used adenosine aptamer DNA and ThT to detect adenosine. As shown in Figure 1A, the fluorescence of the system decreased after the addition of adenosine. Triton X-100 had no obvious effect on the fold change in the fluorescence of the system, although the overall fluorescence was approximately 30% lower in the presence of the surfactant (Figure 5A). Next, we monitored the fluorescence kinetics of the samples containing adenosine aptamer and 100 μM adenosine for 30 min (Figure 5B). In the absence of Triton X-100, the fluorescence of the system decreased slowly before 20 min, and then decreased rapidly after 20 min. After 30 min, the fluorescence signal dropped by 41%. The fluorescence of the system did not change significantly after 15 min in the presence of 0.01% Triton X-100. Thus, the addition of Triton X-100 can improve signal reliability in this case.

3.6. Evaluation of the Cortisol Aptamer

Finally, we used the CSS.1-42 aptamer to detect cortisol (Figure 6A) [33,34]. Our group recently showed that SGI can stain this aptamer and cortisol binding results in a moderate fluorescence increase [34]. Triton X-100 had no significant effect on the fold change in fluorescence of the system (18.0% without versus 28.4% with Triton X-100, Figure 6B), although, again, the overall fluorescence was lower in the presence of the surfactant. We then performed a 30 min fluorescence stability assay on samples containing 5 μM cortisol in a 96-well plate (Figure 6C). In the absence of Triton X-100, the fluorescence of the sample dropped rapidly in the first 10 min and decreased by 24% after 30 min. In contrast, the fluorescence signal of the system was more stable after the addition of Triton X-100 and decreased by only 5.7% in 30 min. This stable signal can make cortisol detection more accurate.

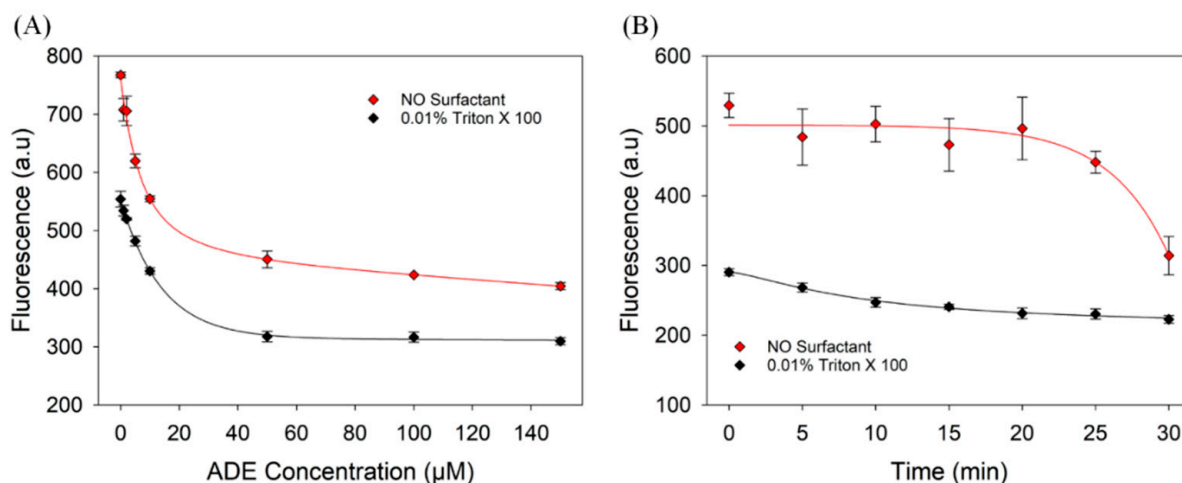


Figure 5. (A) Titration curve of 1 μM adenosine aptamer by adenosine without and with 0.01% Triton X-100. (B) Effect of Triton X-100 on signal stability of the adenosine aptamer/ThT system in the presence of 100 μM adenosine.

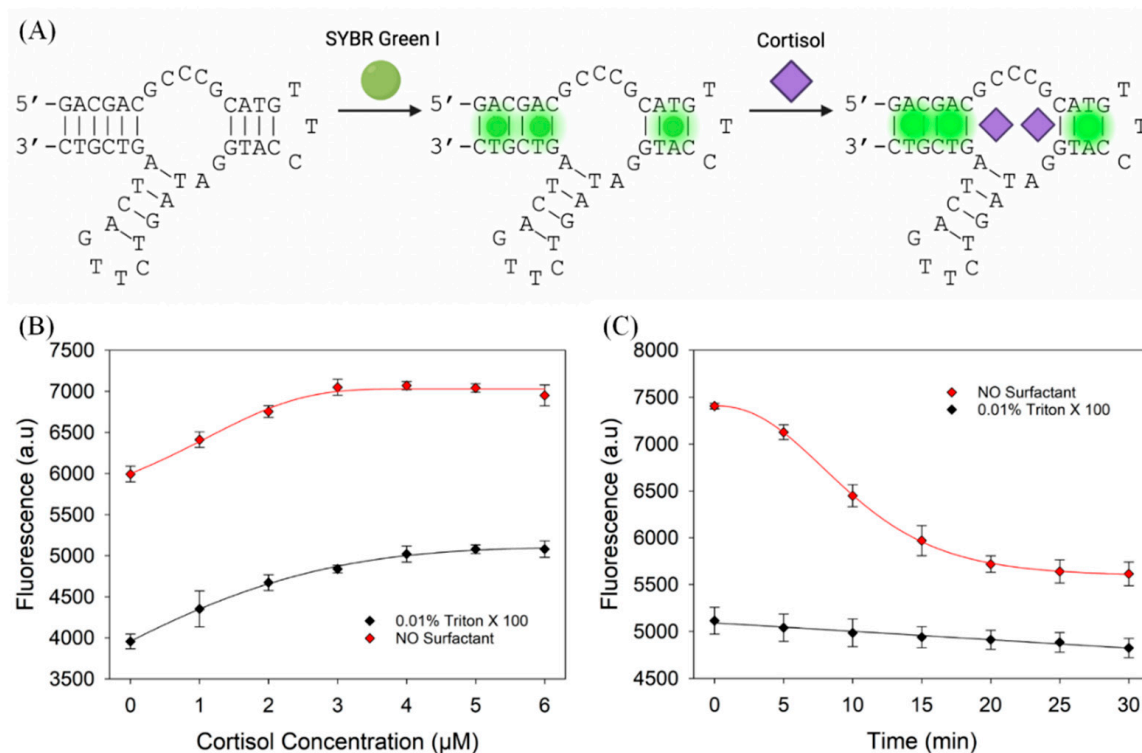


Figure 6. (A) The scheme of cortisol binding to its aptamer detected by SYBR Green I. Initially, the combination of SGI and aptamer produces weak fluorescence, and after the addition of cortisol, aptamer–cortisol binding results in enhanced fluorescence. (B) Titration curve of 1 μM CSS.1-42 with cortisol with and without Triton X-100. (C) Effect of Triton X-100 on signal stability of CSS.1-42 Apt-SGI-cortisol titration.

4. Conclusions

Recently, many new aptamers have been reported, [33,35–37] and the development of reliable binding assays is ever more important. [1,2,38] In this work, we examined the stability of the fluorescence signal of various DNA staining dyes with various aptamers in both polystyrene microplates and a quartz cuvette. A time-dependent fluorescence drop was observed in most cases, especially in the microplates, attributable to the adsorption of cationic DNA-staining dyes to the walls of the vessels. We can classify the purpose of

such experiments into two types. First, for qualitative measurement to answer questions such as whether a DNA sequence is an aptamer or not; using carefully designed control sequences and control target molecules is very important to confirm that the change in fluorescence is due to aptamer binding instead of other events, such as dye adsorption. Even in the presence of nonspecific dye adsorption, aptamer binding might still generate a greater signal change. Using a single aptamer sequence cannot generate reliable answers. The best control sequences would be those with a point mutation. As can be seen from this study, the fluorescence response of different DNA can be very drastic to different DNA staining dyes. So, using a totally unrelated scramble sequence is less reliable than using mutants of aptamers.

Second, for quantitative measurements to obtain values such as K_d and kinetic information, the dye adsorption problem can be mitigated using either a long waiting time with agitation or by adding a surfactant such as Triton X-100. Using this surfactant, we tested three aptamers for Hg^{2+} , adenosine, and cortisol. In each case, a more stable signal was observed with the surfactant, although a target concentration-dependent fluorescence change was achieved even without the surfactant. In addition, using a quartz cuvette is recommended over a plastic microplate to achieve more accurate K_d measurement.

Overall, we articulated the signal stability problem of DNA staining dye-based aptamer binding assays and provided a few solutions to solve this problem to generate more reliable measurements and biosensors.

Author Contributions: Conceptualization, J.L.; methodology, J.L., H.Z. and A.Z.L.; formal analysis, J.L., H.Z. and A.Z.L.; investigation, H.Z. and A.Z.L.; data curation, H.Z. and A.Z.L.; writing—original draft preparation, H.Z. and A.Z.L.; writing—review and editing, J.L.; supervision, J.L.; project administration, J.L.; funding acquisition, J.L. All authors have read and agreed to the published version of the manuscript.

Funding: This research was funded by the Discovery Grant of the Natural Sciences and Engineering Research Council of Canada (NSERC).

Institutional Review Board Statement: Not applicable.

Informed Consent Statement: Not applicable.

Data Availability Statement: Not applicable.

Conflicts of Interest: The funders had no role in the design of the study; in the collection, analyses, or interpretation of data; in the writing of the manuscript; or in the decision to publish the results.

References

1. Daems, E.; Moro, G.; Campos, R.; De Wael, K. Mapping the gaps in chemical analysis for the characterisation of aptamer-target interactions. *TrAC Trends Anal. Chem.* **2021**, *142*, 116311. [[CrossRef](#)]
2. McKeague, M.; De Girolamo, A.; Valenzano, S.; Pascale, M.; Ruscito, A.; Velu, R.; Frost, N.R.; Hill, K.; Smith, M.; McConnell, E.M.; et al. Comprehensive Analytical Comparison of Strategies Used for Small Molecule Aptamer Evaluation. *Anal. Chem.* **2015**, *87*, 8608–8612. [[CrossRef](#)]
3. Yu, H.; Alkhamis, O.; Canoura, J.; Liu, Y.; Xiao, Y. Advances and Challenges in Small-Molecule DNA Aptamer Isolation, Characterization, and Sensor Development. *Angew. Chem. Int. Ed.* **2021**, *60*, 16800–16823. [[CrossRef](#)]
4. He, L.; Huang, R.; Xiao, P.; Liu, Y.; Jin, L.; Liu, H.; Li, S.; Deng, Y.; Chen, Z.; Li, Z.; et al. Current signal amplification strategies in aptamer-based electrochemical biosensor: A review. *Chin. Chem. Lett.* **2021**, *32*, 1593–1602. [[CrossRef](#)]
5. Liu, J.; Cao, Z.; Lu, Y. Functional Nucleic Acid Sensors. *Chem. Rev.* **2009**, *109*, 1948–1998. [[CrossRef](#)] [[PubMed](#)]
6. Zhang, P.; Qin, K.; Lopez, A.; Li, Z.; Liu, J. General Label-Free Fluorescent Aptamer Binding Assay Using Cationic Conjugated Polymers. *Anal. Chem.* **2022**, *94*, 15456–15463. [[CrossRef](#)]
7. Zhao, Y.; Gao, B.; Sun, P.; Liu, J.; Liu, J. Metal and pH-Dependent Aptamer Binding of Tetracyclines Enabling Highly Sensitive Fluorescence Sensing. *Biosensors* **2022**, *12*, 717. [[CrossRef](#)]
8. Li, L.-L.; Ge, P.; Selvin, P.R.; Lu, Y. Direct Detection of Adenosine in Undiluted Serum Using a Luminescent Aptamer Sensor Attached to a Terbium Complex. *Anal. Chem.* **2012**, *84*, 7852–7856. [[CrossRef](#)] [[PubMed](#)]
9. Lu, C.; Lopez, A.; Zheng, J.; Liu, J. Using the Intrinsic Fluorescence of DNA to Characterize Aptamer Binding. *Molecules* **2022**, *27*, 7809. [[CrossRef](#)]

10. Yeasmin Khusbu, F.; Zhou, X.; Chen, H.; Ma, C.; Wang, K. Thioflavin T as a fluorescence probe for biosensing applications. *TrAC Trends Anal. Chem.* **2018**, *109*, 1–18. [[CrossRef](#)]
11. NK, R.; Kamali, R.V.; Gorthi, S.S. A rapid aptamer-based fluorescence assay for the detection of lipopolysaccharides using SYBR Green I. *Luminescence* **2021**, *36*, 1632–1637.
12. Xiao, S.; Sun, L.; Lu, J.; Dong, Z. A label-free aptasensor for rapid detection of clenbuterol based on SYBR Green I. *New J. Chem.* **2022**, *46*, 16177–16182. [[CrossRef](#)]
13. Li, B.; Dong, S.; Wang, E. Homogeneous Analysis: Label-Free and Substrate-Free Aptasensors. *Chem. Asian J.* **2010**, *5*, 1262–1272. [[CrossRef](#)] [[PubMed](#)]
14. Suss, O.; Motiei, L.; Margulies, D. Broad Applications of Thiazole Orange in Fluorescent Sensing of Biomolecules and Ions. *Molecules* **2021**, *26*, 2828. [[CrossRef](#)]
15. Zhang, P.; Zandieh, M.; Ding, Y.; Wu, L.; Wang, X.; Liu, J.; Li, Z. A Label-Free, Mix-and-Detect ssDNA-Binding Assay Based on Cationic Conjugated Polymers. *Biosensors* **2023**, *13*, 122. [[CrossRef](#)] [[PubMed](#)]
16. Zhang, F.; Liu, J. Label-Free Colorimetric Biosensors Based on Aptamers and Gold Nanoparticles: A Critical Review. *Anal. Sens.* **2021**, *1*, 30–43. [[CrossRef](#)]
17. Liu, X.; He, F.; Zhang, F.; Zhang, Z.; Huang, Z.; Liu, J. Dopamine and Melamine Binding to Gold Nanoparticles Dominates Their Aptamer-based Label-free Colorimetric Sensing. *Anal. Chem.* **2020**, *92*, 9370–9378. [[CrossRef](#)]
18. Zhang, F.; Huang, P.-J.J.; Liu, J. Sensing Adenosine and ATP by Aptamers and Gold Nanoparticles: Opposite Trends of Color Change from Domination of Target Adsorption Instead of Aptamer Binding. *ACS Sens.* **2020**, *5*, 2885–2893. [[CrossRef](#)]
19. Zahraee, H.; Khoshbin, Z.; Ramezani, M.; Alibolandi, M.; Abnous, K.; Taghdisi, S.M. A tag-free fluorescent aptasensor for tobramycin detection using a hybridization of three aptamer strands and SYBR Green I dye. *Spectrochim. Acta Part A Mol. Biomol. Spectrosc.* **2023**, *290*, 122305. [[CrossRef](#)]
20. Kong, L.; Xu, J.; Xu, Y.; Xiang, Y.; Yuan, R.; Chai, Y. A universal and label-free aptasensor for fluorescent detection of ATP and thrombin based on SYBR Green Idye. *Biosens. Bioelectron.* **2013**, *42*, 193–197. [[CrossRef](#)]
21. Sarpong, K.; Datta, B. Nucleic-Acid-Binding Chromophores as Efficient Indicators of Aptamer-Target Interactions. *J. Nucleic Acids* **2012**, *2012*, 247280. [[CrossRef](#)] [[PubMed](#)]
22. Zipper, H.; Brunner, H.; Bernhagen, J.; Vitzthum, F. Investigations on DNA intercalation and surface binding by SYBR Green I, its structure determination and methodological implications. *Nucleic Acids Res.* **2004**, *32*, e103. [[CrossRef](#)] [[PubMed](#)]
23. Kolbeck, P.J.; Vanderlinden, W.; Gemmecker, G.; Gebhardt, C.; Lehmann, M.; Lak, A.; Nicolaus, T.; Cordes, T.; Lipfert, J. Molecular structure, DNA binding mode, photophysical properties and recommendations for use of SYBR Gold. *Nucleic Acids Res.* **2021**, *49*, 5143–5158. [[CrossRef](#)]
24. Huizenga, D.E.; Szostak, J.W. A DNA Aptamer That Binds Adenosine and ATP. *Biochemistry* **1995**, *34*, 656–665. [[CrossRef](#)] [[PubMed](#)]
25. Li, Y.; Liu, J. Aptamer-based strategies for recognizing adenine, adenosine, ATP and related compounds. *Analyst* **2020**, *145*, 6753–6768. [[CrossRef](#)] [[PubMed](#)]
26. Zhang, Z.; Oni, O.; Liu, J. New insights into a classic aptamer: Binding sites, cooperativity and more sensitive adenosine detection. *Nucleic Acids Res.* **2017**, *45*, 7593–7601. [[CrossRef](#)] [[PubMed](#)]
27. Peterson, A.M.; Jahnke, F.M.; Heemstra, J.M. Modulating the Substrate Selectivity of DNA Aptamers Using Surfactants. *Langmuir* **2015**, *31*, 11769–11773. [[CrossRef](#)]
28. Liu, B.; Huang, P.-J.J.; Zhang, X.; Wang, F.; Pautler, R.; Ip, A.C.F.; Liu, J. Parts-per-Million of Polyethylene Glycol as a Non-Interfering Blocking Agent for Homogeneous Biosensor Development. *Anal. Chem.* **2013**, *85*, 10045–10050. [[CrossRef](#)] [[PubMed](#)]
29. Karthikeyan, N.; Giridhar, V.; Vasudevan, D. Surfactant effects on methanol oxidation at Pt-Ru/C coated glassy carbon electrode. *J. Solid State Electrochem.* **2010**, *14*, 877–881. [[CrossRef](#)]
30. Lavkush Bhaisare, M.; Pandey, S.; Shahnawaz Khan, M.; Talib, A.; Wu, H.-F. Fluorophotometric determination of critical micelle concentration (CMC) of ionic and non-ionic surfactants with carbon dots via Stokes shift. *Talanta* **2015**, *132*, 572–578. [[CrossRef](#)] [[PubMed](#)]
31. Bak, A.; Podgorska, W. Investigation of drop breakage and coalescence in the liquid-liquid system with nonionic surfactants Tween 20 and Tween 80. *Chem. Eng. Sci.* **2012**, *74*, 181–191. [[CrossRef](#)]
32. Wang, J.; Liu, B. Highly sensitive and selective detection of Hg²⁺ in aqueous solution with mercury-specific DNA and Sybr Green I. *Chem. Commun.* **2008**, *39*, 4759–4761. [[CrossRef](#)] [[PubMed](#)]
33. Yang, K.-A.; Chun, H.; Zhang, Y.; Pecic, S.; Nakatsuka, N.; Andrews, A.M.; Worgall, T.S.; Stojanovic, M.N. High-Affinity Nucleic-Acid-Based Receptors for Steroids. *ACS Chem. Biol.* **2017**, *12*, 3103–3112. [[CrossRef](#)]
34. Niu, C.; Ding, Y.; Zhang, C.; Liu, J. Comparing two cortisol aptamers for label-free fluorescent and colorimetric biosensors. *Sens. Diagn.* **2022**, *1*, 541–549. [[CrossRef](#)]
35. Yu, H.; Luo, Y.; Alkhamis, O.; Canoura, J.; Yu, B.; Xiao, Y. Isolation of Natural DNA Aptamers for Challenging Small-Molecule Targets, Cannabinoids. *Anal. Chem.* **2021**, *93*, 3172–3180. [[CrossRef](#)]
36. Huang, P.-J.J.; Liu, J. Simultaneous Detection of L-Lactate and D-Glucose Using DNA Aptamers in Human Blood Serum. *Angew. Chem. Int. Ed.* **2023**, *62*, e20221287. [[CrossRef](#)]

37. Niu, C.; Zhang, C.; Liu, J. Capture-SELEX of DNA Aptamers for Estradiol Specifically and Estrogenic Compounds Collectively. *Environ. Sci. Technol.* **2022**, *56*, 17702–17711. [[CrossRef](#)]
38. Zhao, Y.; Yavari, K.; Liu, J. Critical evaluation of aptamer binding for biosensor designs. *TrAC Trends Anal. Chem.* **2022**, *146*, 116480. [[CrossRef](#)]

Disclaimer/Publisher's Note: The statements, opinions and data contained in all publications are solely those of the individual author(s) and contributor(s) and not of MDPI and/or the editor(s). MDPI and/or the editor(s) disclaim responsibility for any injury to people or property resulting from any ideas, methods, instructions or products referred to in the content.